CHARACTERISTICS OF LOCAL BUBBLE PARAMETERS OF SUBCOOLED BOILING FLOW IN AN ANNULUS

B.J. Yun*[1], B.U.Bae[2], W.M.Park[1], D.J.Euh[1], G.C.Park[2], C-.H. Song[1]

[1]Thermal Hydraulics Safety Research Department, Korea Atomic Energy Research Institute, Korea
**Phone: +82 (42) 868 8756, Fax: +82 (42) 868 8362, E-Mail: bjyun@kaeri.re.kr*
[2]Department of Nuclear Eng., Seoul National University, Korea

Abstract

Subcooled boiling phenomena have become important for the design, operation and safety analysis of a nuclear power plant. For a better prediction of these subcooled boiling phenomena, an experimental study was carried out in the SUBO (Subcooled boiling) test facility. The test section is a vertical annulus with a heater rod at the center of a channel. For the measurement of the local bubble parameters, double sensor optical fiber probes were applied at six elevations. Six cases of test matrix were chosen for the parametric study of the heat flux, mass flux and inlet subcooling. Void fraction, interfacial area concentration, Sauter mean diameter and bubble velocity were measured at 12 radial locations at each elevation. The local bubble parameters show well three-dimensional characteristics and propagation of a void fraction and an interfacial area concentration along the test section in a subcooled boiling flow. The characteristics of the SUBO test are that it has a very long test channel and can cover a wide range of test conditions compared to previous available data. The present data is expected to be valuable for a benchmark validation and model development of the CFD codes or existing safety analysis codes.

1. INTRODUCTION

Subcooled boiling becomes one of the crucial phenomena for the design, operation and safety analysis of a nuclear power plant. However, it has been found that most of the existing best estimate safety analysis codes have a weakness in the prediction of subcooled boiling phenomena, especially in a low pressure condition. Recently, an issue has been boron deposition on the surface of nuclear fuel rods in which a subcooled boiling occurs during the normal operation of a PWR (Pressurized Water Reactor). In addition, the safety analysis for the APR1400 (Korean advanced power reactor) showed that subcooled boiling phenomena in the reactor downcomer results in a reduction of the reflood flow rate for the core cooling during a postulated large break loss of coolant accident (LBLOCA). (Yun, 2006, Song, 2007) For a better prediction of these subcooled boiling phenomena, development of advanced analysis tools or an improvement of the related models for the existing prediction tools is still required. For this, experimental work for the subcooled boiling phenomena is indispensable.

Zeitoun (1994) conducted a subcooled boiling test in a high heat flux condition, however the test section for the boiling heat transfer was short in length. Roy (2002) studied the turbulent structure of a two-phase flow behavior in the R-113 loop and validated the ASTRID code. At Purdue University, Situ (2004) measured the radial distribution of the local two-phase flow parameters and utilized the data for verifying the model for a distribution parameter and co-variance in a drift flux model. In Seoul National University (SNU), Lee (2002) and Kim (2004) performed subcooled boiling experiments and analyses with a commercial CFD code (CFX) or a thermal hydraulic system analysis code (RELAP). From the literature for the subcooled boiling experiments described above, it can be interpreted that the experimental data base for extended test conditions of a subcooled boiling flow are required for an advanced analysis of a multi-dimensional two-phase flow.

In this study, subcooled boiling test was performed in the SUBO (*SU*bcooled *BO*iling) test facility to extend the data base for a higher mass flux and heat flux condition. From the experiments, the characteristics of the local bubble parameters in a subcooled boiling flow were investigated.

2. EXPERIMENTAL FACILITY

2.1 Test facility

In order to investigate the subcooled boiling phenomena by measuring the local bubble parameters, the SUBO facility was constructed as shown in Fig. 1 (Yun, 2008). The test facility consists of a test section, a preheater, a storage tank, a separator, two pumps and two heat exchangers. Demineralised water in the storage tank is injected through the preheater to the test section by a circulating pump, where the inlet temperature of the water is controlled by a preheater. The separator is connected to the outlet pipe of the test section for a phase separation of a two-phase flow. The separated water and steam phases respectively are cooled and condensed by two heat exchangers. The temperature of the water in the storage tank is controlled by the heat removal rates of these heat exchangers. The injected water mass flow rate of the test facility is controlled by a control valve and the system pressure is controlled by an air injection and venting system.

The test section of the facility is a vertically arranged annulus with an in-direct heater rod at the channel center as depicted in Fig. 2. The inner diameter of the test section is 35.5mm and the outer diameter of the heater rod is 10.02mm. The heater rod consists of three parts. The first part is an unheated section with 222mm length for regulating the water condition at the inlet, the second part is a heated section with 3098mm length for the simulation of a boiling, and the third part is an unheated section with 800mm length for bubble condensation at the top region. The maximum available mass flux and heat flux of the SUBO are 6000 kg/m^{2}s and 934 kW/m^2, respectively. The maximum operational pressure of the test facility is 500 kPa.

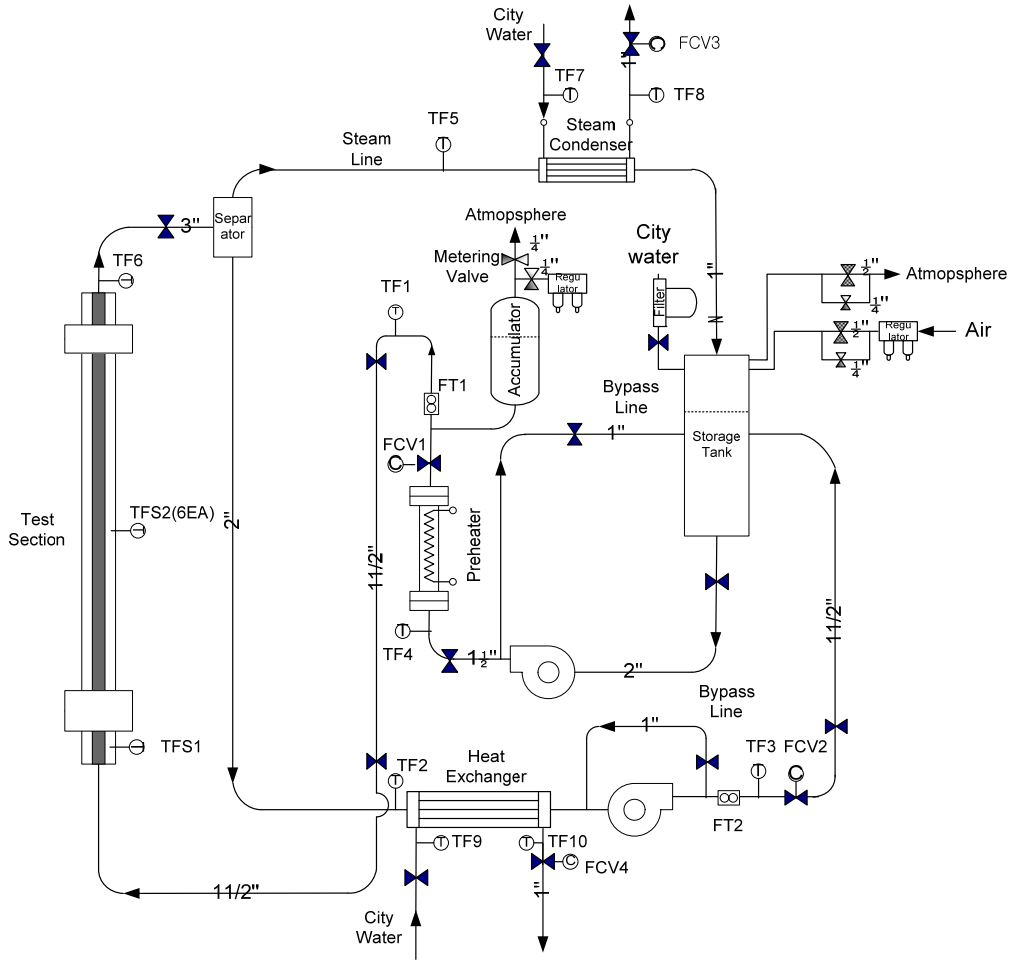

Fig. 1 Test loop of the SUBO facility

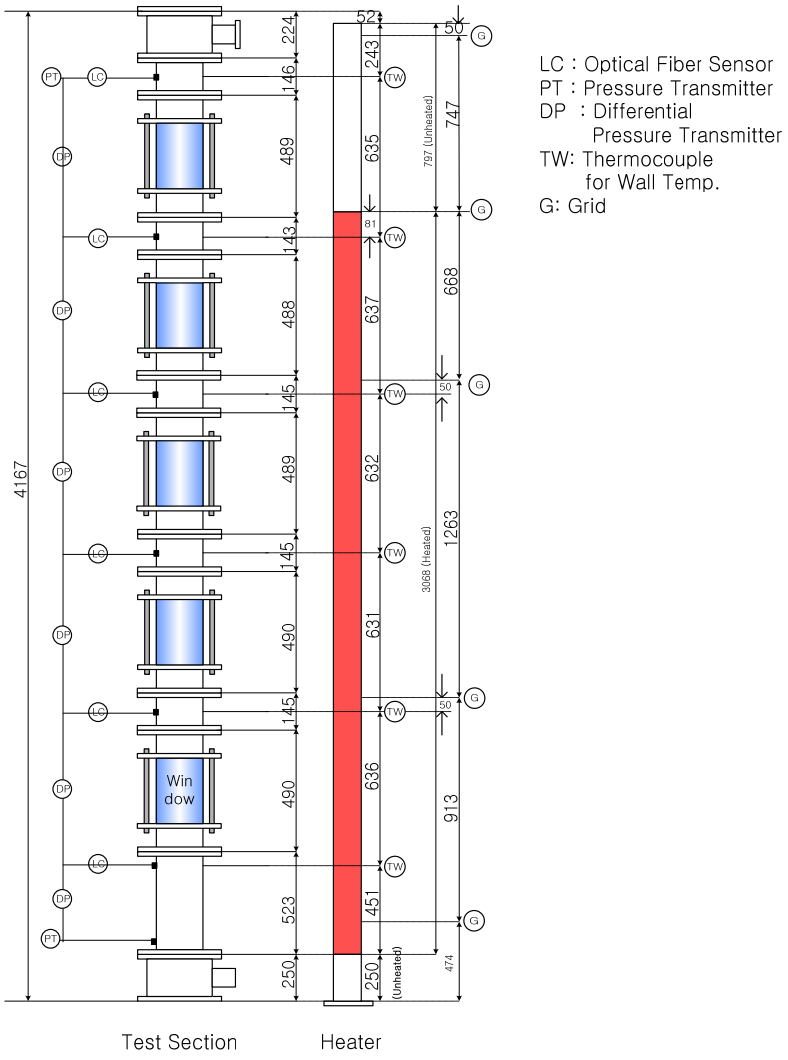

Fig. 2 Test section of the SUBO facility

In the test loop, several kinds of commercially available instruments are installed for the measurements of total mass flow rate, static and differential pressures, and the fluid temperature. In addition, a total 6 elevations are chosen for the measurement of the local two-phase flow parameters along the test section. At each elevation, a thermocouple is installed to measure the surface temperature of a heater rod. At the top and bottom of the test section, two pressure transmitters are installed. Moreover, six differential pressure transmitters are installed between the two pressure transmitters to obtain the pressure distributions along the axial direction of the test section. The instruments including their detailed locations for the test section are shown in Fig.2. Types of installed instruments and their uncertainties are summarized in Table 1. The special instrumentation for the local bubble parameters is described in the following session.

2.2 Measurement of the local bubble parameters

In order to quantify the complicated bubble behavior in a two-phase flow condition, a double sensor optical fiber probe has been applied for a measurement of the local void fraction, the bubble velocity, the Sauter mean diameter, and the interfacial area concentration. Fig. 3 shows the schematics of the double sensor optical fiber probe which was developed in-house. The sensing tip of an optical probe can distinguish a phase at a local position by the characteristics of the light penetration and reflection between the gas and liquid phases. Outer diameter of the optical fiber is 125 μm and the diameter of the sensing tip is less than 30 μm.

Table 1 Type and uncertainty of the instruments

Parameter	Instrument	Location	Uncertainty
Mass flow	Coriolis meter	Inlet and outlet of test section	0.3% of read value
System pressure	SMART-type pressure transmitter	Top and bottom of test section	1 kPa
Differential pressure (DP)	SMART-type DP transmitter	Uniformly spaced along test section	5 Pa
Temperature	K-type thermocouple	Inlet and outlet of test section	2.2K
Heater power	Power meter	-	0.35% of read value

Its small diameter can minimize the flow disturbance which can be resulted by the sensor and make it possible to detect very small bubbles. For the measurement of the propagation of the local bubble parameters, two optical fiber sensors were applied at the six elevations along the test section. Among them, five (L/D_h=17.6, 42.5, 66.4, 91.7, 116.2) were installed in the heated region and one (L/D_h=141.2) was installed in the unheated condensation region. The radial distribution of the local bubble parameters were obtained at 12 locations between the heater rod and the outer pipe at each elevation, so that a multi-dimensional bubble behavior could be understood. The uncertainties of a local void fraction and a bubble velocity using the local probe methodology are evaluated to be 6.1% and 3.01%, respectively, from the air/water benchmark test (Euh *et al*. 2005).

3. EXPERIMENT

The characteristics of the SUBO facility are that it has a capacity for simulating experimental conditions with a wide range of heat and mass fluxes with a longer vertical channel when it is compared with other previous test facilities. In the present test, a total of six test matrixes were chosen for the parametric study of the heat flux, the mass flux and the degree of inlet subcooling on the base case. The test conditions of each test matrix are tabulated in Table 2. Outlet pressure was kept at about 155kPa during all of the tests. When compared to the Base case, Q1 and Q2 cases are used to investigate the effect of a heat flux. Moreover, in order to observe the subcooled boiling phenomena according to various conditions, V1 and V2 cases have a higher mass flux rather

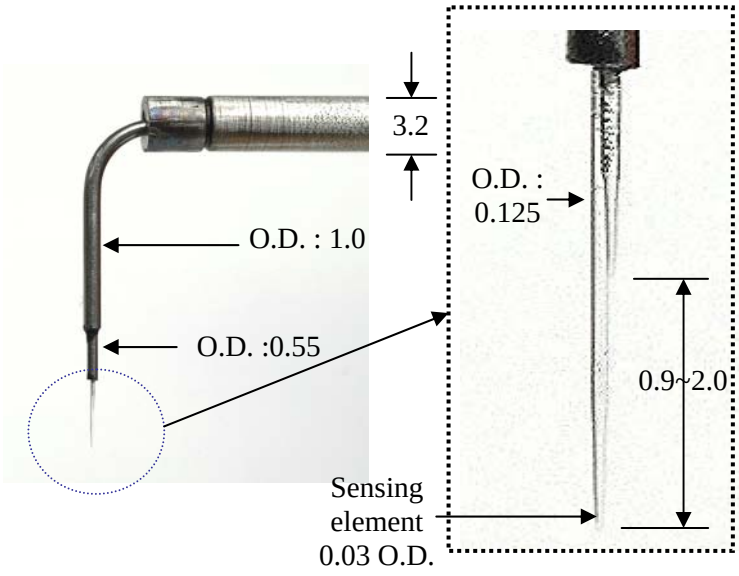

Fig. 3 Double sensor optical fiber probe (Dimensions in mm)

Table 2 Summary of the experimental conditions according to the test matrixes

Case	Heat flux (kW/m^2)	Mass flux (kg/m^2s)	Inlet subcooling (K)	Inlet pressure (kPa)	Outlet pressure (kPa)
Base	470.6	1132.6	19.1	192.9	157.3
Q1	363.7	1119.6	19.0	192.7	156.7
Q2	563.0	1126.9	18.3	188.9	155.7
V1	465.7	2126.5	19.6	196.9	156.9
V2	567.9	2128.8	19.5	197.6	158.0
T1	465.5	1103.9	29.6	190.7	155.0

than the base case and the T1 case has a higher inlet subcooling condition for a given base mass flux condition. One of the main purposes of the present test matrixes is to achieve a database for a validation and benchmarking of developed CFD style codes. To quantify the heat loss to the atmosphere for the above test matrixes, a series of heat loss tests was performed in a single phase flow condition. It showed that the maximum heat release rate was estimated to be 2.5 kW for all the cases.

4. EXPERIMENTAL RESULTS

4.1Visual observation

During present experiments, the phenomena in the test section were recorded with a high-speed camera. Photographs at three elevations during the Base case experiment are shown in Fig. 4. At the elevation around L/D_h=30, a wall voidage region was observed on the heated wall, where the bubble from the nucleation sites could not contribute a significant void generation due to its rapid condensation in a highly subcooled water. As it moves to the downstream along the heating rod, a net vapor generation occurred as depicted in Fig. 4(b). In this region, a large bubble appeared by coalescences among the departed bubbles on the heated wall and then they were lifted off the surface. After passing the heated section of a heater rod, the number density and interfacial area of the bubbles were decreased rapidly due to a bubble condensation.

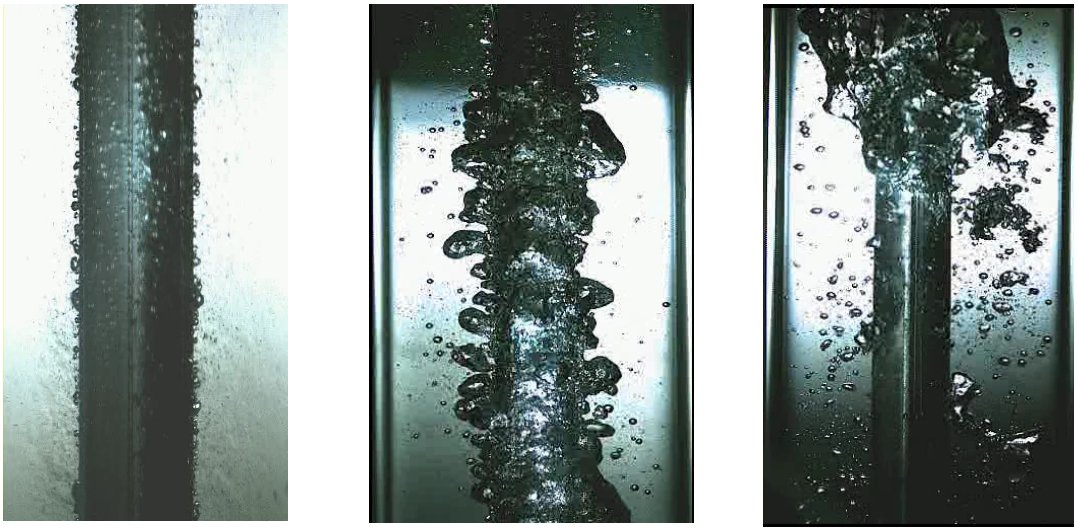

(a) Wall voidage (L/D_h=30) (b) Net vapor generation (L/D_h=79) (c) Condensation (L/D_h=129)

Fig. 4 Visual observations along the test section

4.2 Local bubble parameters

The radial profile and axial propagation of the local void fraction according to the heat flux, the mass flux and the inlet subcooling are shown in figure 5. In the figure, $r^* = 0$ corresponds to the surface of a heating rod, whereas $r^* = 1$ is the inner surface of an outer pipe. Measurement positions from L/D_h=17.6 to L/D_h=116.2 existed in the heated section, while the position at L/D_h=141.3 was located in the condensation region.

One of the representative characteristics of a subcooled boiling is the existence of two different flow regions in a flow channel, which results from a thermal non-equilibrium between two phases. One is a bubbly boundary layer region and the other is a subcooled liquid core region. It was already found from previous work that the thickness of the bubbly boundary layer at each inlet subcooling, mass flux, and wall heat flux condition is highly dependent on the bubble size (Jiji & Clark, 1964), which is determined by a balance of the coalescence and condensation rates. In the figure, the thickness of a bubbly boundary layer can be found with the distance from the heater surface to the radial position where the void fraction is zero. Figure 5 clearly shows that the thickness of the bubbly boundary layer increases as it moves upward for a given flow condition, and it increases as the applied heat flux increases, whereas it decreases as inlet subcooling or mass flux increases. Naturally, the distribution of the local void fraction is closely related with the behaviour of the bubbly boundary layer. As shown in the figure, the local void fraction decreases from the surface of the heating rod to the subcooled liquid core. In addition, the peak of local void fraction appears adjacent to the surface of heating rod and its magnitude tends to increase as the inlet subcooling or mass flux decreases. The void peaking near the heating rod is quite different from the wall void peaking phenomena, which are observable in the air-water experiments. The wall peaking of the local void fraction in the air-water flow is due to a migration of the bubbles toward the wall, and thereby the bubble number density profile follows the

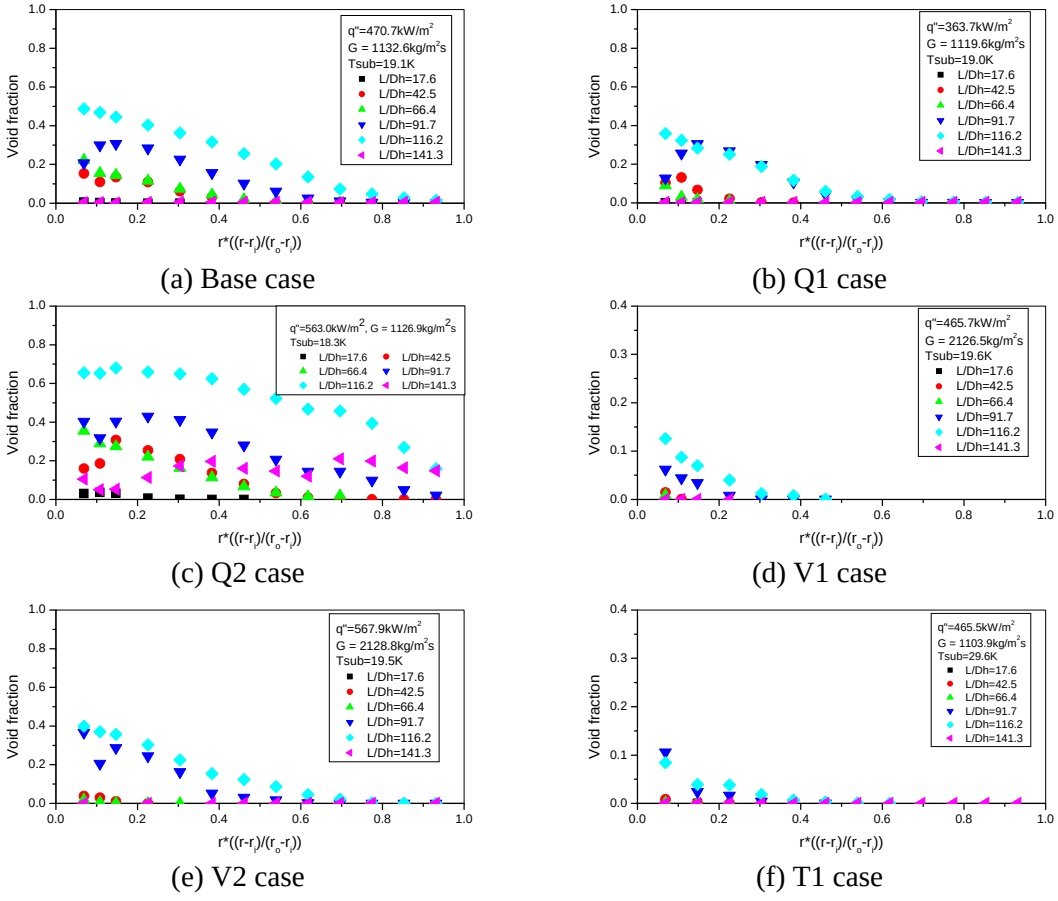

(a) Base case (b) Q1 case

(c) Q2 case (d) V1 case

(e) V2 case (f) T1 case

Fig. 5 Void fraction distribution according to the heat flux, the mass flux and the inlet subcooling

trend of the local void fraction. However, the void peaking near the heating rod during the subcooled boiling are explicitly due to the large number of bubbles which are generated from the boiling sites on the surface of the heating rod and coming from the upstream direction. And the highly populated bubbles near the heater rod region condense as they move to the subcooled liquid core region by an interfacial heat transfer. Present data shows the qualitative trend of this subcooled boiling phenomenon well in almost all cases. Comparison between the void fraction in the Base, Q1, and Q2 cases showed a dependency of the void propagation behaviour on the heat flux condition. Q1 case with a lower heat flux indicated a lower void fraction than the Base case and the bubbly boundary layer could not cover the whole flow channel even at the L/D_h=116.2 position. Q2 case with a higher heat flux indicated a larger void generation and a thicker bubbly boundary layer than the Base case or Q1 case, where the peak void fraction at L/D_h=116.2 was around 0.7. On the other hand, results of V1 and V2 cases revealled the effect of an increased mass flux when compared with the Base and Q2 cases, respectively. Larger mass flow in the channel reduced the enthalpy rise of the fluid while flowing through the heated section, so that the thickness of the bubbly boundary layer was reduced by a decreased void generation. T1 case had a larger inlet subcooling and it decreased the amount of vapor generation, so that a meaningful void fraction was only detected at L/D_h=91.7 and L/D_h=116.2.

Figure 6 shows the radial distribution and axial propagation of the interfacial area concentration. As shown in the figure 6, the trend of the interfacial area concentration was closely related to the void fraction. That is, the radial distribution of the interfacial area concentration exhibits a similar behaviour to that of the local void fraction. In addition, their trends for the heat flux, mass flux, and degree of inlet subcooling follow those of the local void fraction. However, it should be noted that a sharp increase of the interfacial area concentration always existed near the heated wall and its maximum value which was observed adjacent to the wall was not in an order of the heated length, L/D_h. That means the coalescences around the heating rod occur more vigorously and this caused a decrease of the interfacial area concentration at a higher elevation.

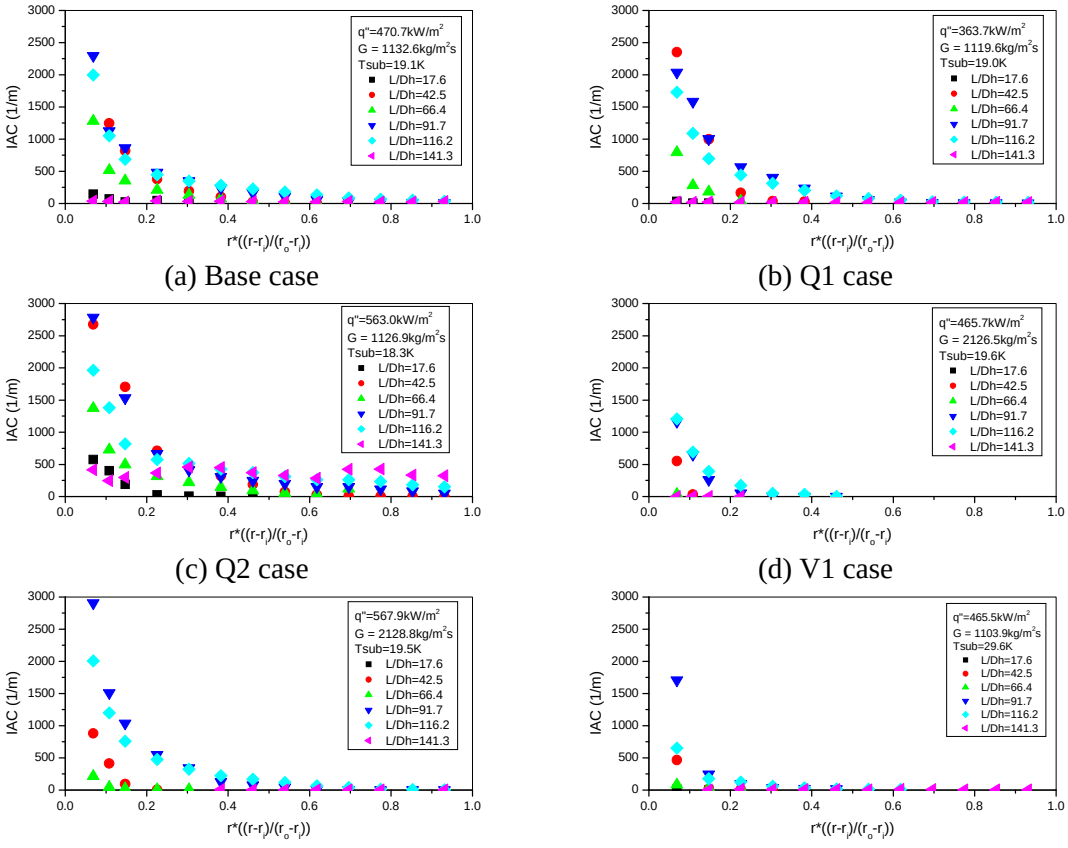

(a) Base case (b) Q1 case

(c) Q2 case (d) V1 case

(e) V2 Case (f) T1 case

Fig. 6 Interfacial area concentration distribution according to the heat flux, the mass flux and the inlet subcooling

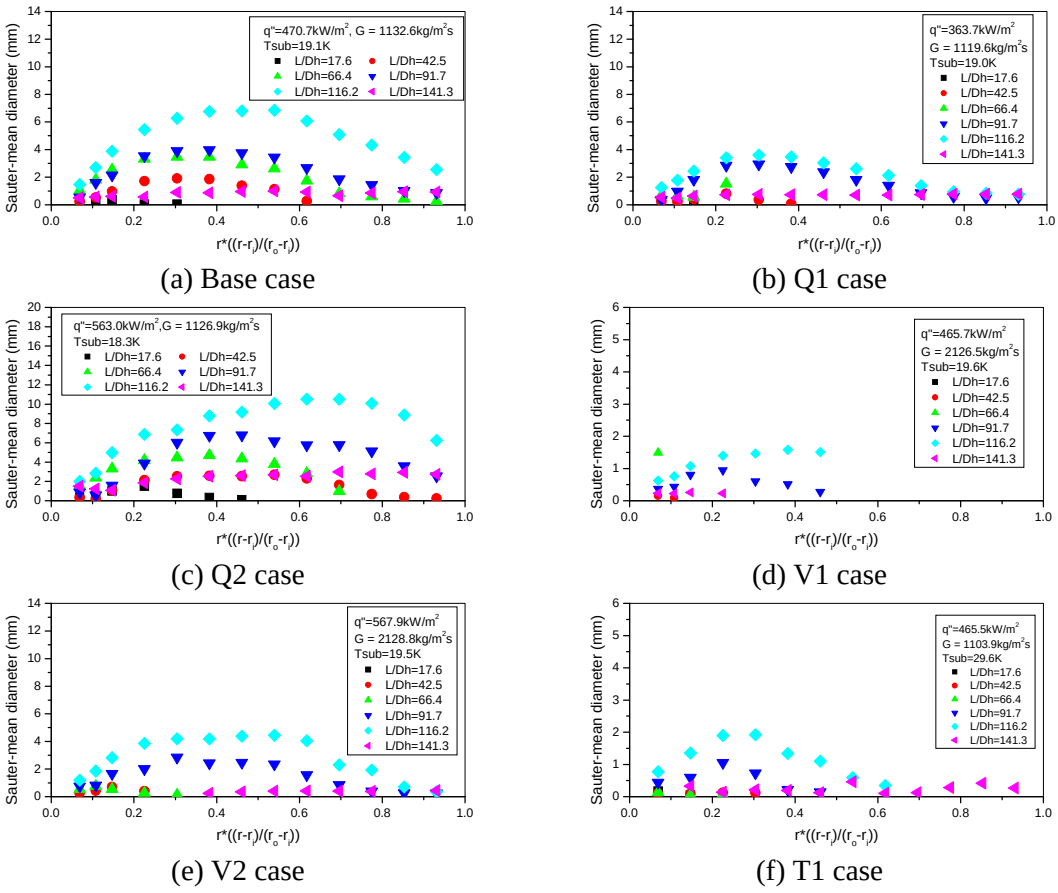

Fig. 7 Sauter mean diameter distribution according to the heat flux, the mass flux and the inlet subcooling

Figure 7 shows the distribution of the Sauter mean diameter. The distribution of the Sauter mean diameter can be explained by the coalescence and condensation of the bubbles. As shown in Fig. 7, the small bubbles coalesce as they move outward from the heater rod wall. Their maximum bubble size was found somewhere inside the bubbly boundary layer and the size decreased due to a condensation as they migrated towards the subcooled liquid core. The heat flux also affected the Sauter mean diameter. Comparison of the Q1 and Q2 cases with Base case shows that the Sauter mean diameter increases at all the measuring positions of the test section and the location of the maximum bubble size moves outward as the heat flux increases. It is caused by a slightly larger detached diameter and a higher coalescence rate by an increased bubble number density. Dependency of the Sauter mean diameter on the mass flux can be understood in detail by comparing the V1 case with the Base case. The Sauter mean diameter decreases as the mass flux increases for a given heat flux. The V2 and Base cases confirm the dependency of the Sauter mean diameter on the heat flux as in the Q1 and Q2 cases. The degree of inlet subcooling effect is found from a comparison of the T1 and Base cases. As shown in the figure, the bubble size decreases by a increased condensation rate as the degree of inlet subcooling increases.

Figure 8 shows an axial development of the bubble velocity distribution. The peak value of the bubble velocity appeared within the central region of the flow channel rather than near the heater rod in which high void fraction was found. It can be explained by the buoyancy effect which results from a bubble size distribution. That is, a bubble with a larger diameter due to the coalescence interactions in the central region could have a larger buoyancy force and be accelerated faster than the small bubbles which exist near the wall. As goes downstream, the bubble velocity is not increased significantly due to the momentum balance between the interfacial friction and the buoyancy force. When compared to the Base, Q1, and Q2 cases in Fig. 8, a high heat flux results in a larger amount of steam generation in the test section and an increased bubble velocity. In the V1 and V2 cases with a larger mass flux,

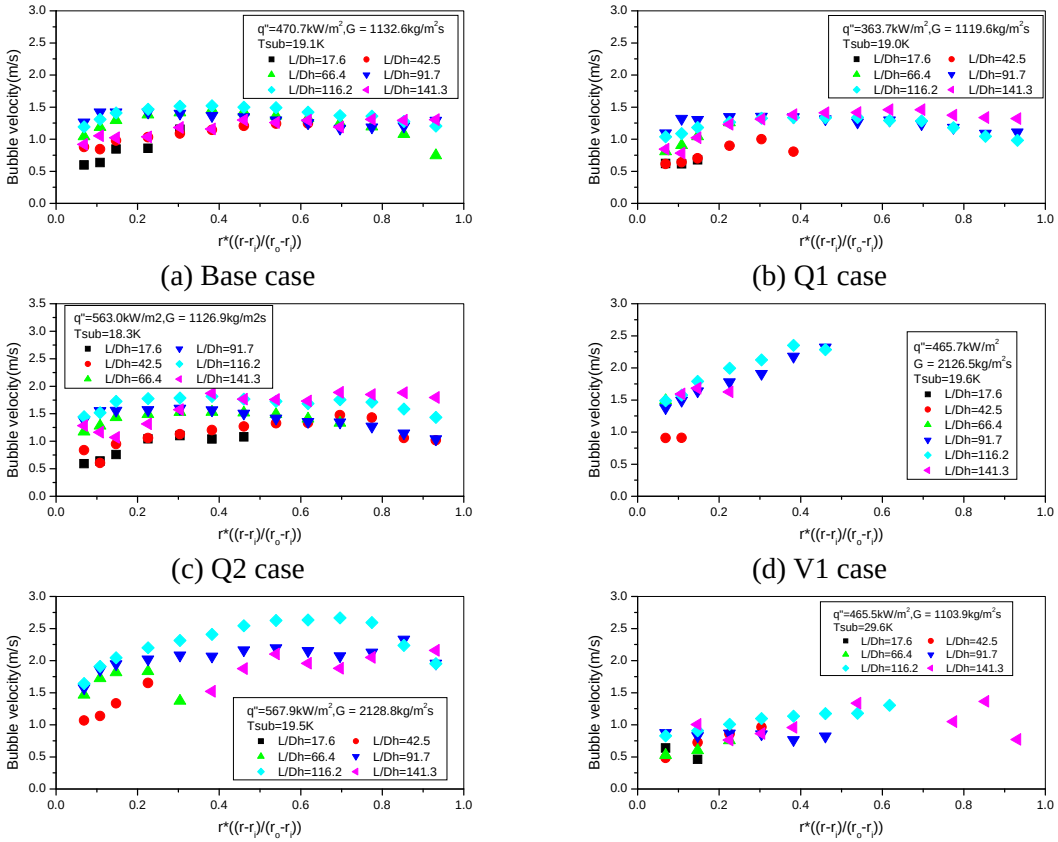

Fig. 8 Bubble velocity distribution according to the heat flux, the mass flux and the inlet subcooling

although the void generation rate was reduced more than in the Base or Q2 case due to a higher subcooling of the fluid, the bubble velocity was increased by the interaction with the liquid phase.

5. CONCLUSION

This study focused on an investigation of a subcooled boiling two-phase flow by measuring the local bubble parameters. Considering a multi-dimensional behavior in a two-phase flow, the axial and radial measurements of the local void fraction, the interfacial area concentration, and the bubble velocity were obtained by using the double sensor optical fiber probes. Test matrix of the SUBO experiment covers the range of 360 ~560 kW/m^2 in heat flux, 1100~ 2130kg/m^{2}s in mass flux, and 19~ 30^o*C* in the degree of inlet subcooling. Experimental results show well the characteristics and the propagation of void fraction and the interfacial area concentration, which are dependent on the heat flux or mass flux conditions. The present data is expected to be suitable for a benchmarking, validation and model development for the CFD codes or conventional safety analysis codes.

In further studies, the distributions of local liquid velocity and temperature will be obtained for the same flow conditions by using a specially designed instrumentation spool, which consists of a local Pitot tube and a thermocouple.

ACKNOLEDGEMENT

The authors wish to express their deep appreciation to Dr. H.K.Cho for his assistance of the experimental work. This study has been carried out under the nuclear R&D program by the Korean Ministry of Education, Science and Technology (MEST).

REFERENCES

Euh, D.J., Yun, B.J, Song, C-.H., “Investigation of the Transport of the Bubble Parameters in Air/Water Flow Conditions”, *ICAPP05*, Seoul, Korea (2005).

Jiji, L.M. and Clark, J.A., "Bubble boundary layer and temperature profiles for forced convection boiling in channel flow", Trans. ASME, J. of Heat Transfer, pp. 50-58 (1964).

Kim, M.O., Kim, S.J., Park, G.C., “The assessment of subcooled boiling models at low pressure,” *Proc. 5th Int’l Conf. on Multiphase Flow (ICMF’04)*, May 30~June 4, Yokohama, Japan (2004).

Lee, T.H., Park, G.C., Lee, D.J., “Local flow characteristics of subcooled boiling flow of water in a vertical concentric annulus”, *Int. J. Multiphase Flow*, 2**8**, 1351-1368 (2002).

Roy, R.P., Kang, S., Zarate, J.A., Laporta, A., “Turbulent subcooled boiling flow – Experiments and simulations”, *ASME J. Heat Transfer*, **124**, 73-93 (2002).

Situ, R., Hibiki, T., Sun, X., Mi, Y., Ishii, M., “Flow structure of subcooled boiling in an internally heated annulus”, *Int. J. Heat Mass Transfer*, **47**, 5351-5364 (2004).

Song, C-.H., Baek, W.P., Park, J.K., “Thermal-hydraulic test and analyses for the APR1400’s development and licensing”, *Nuclear Engineering and Technology*, 39[4], 299-312 (2007).

Yun, B.J., Bae, B.U., Park, W.M., Euh, D.J., Song, C.-H., Park, G.C., "Experimental Study of local bubble parameters of the subcooled boiling flow in a vertical annulus channel", KAERI/TR-3562/2008 (2008).

Yun, B.J, D.J. Euh, Song, C-.H., “Investigation of the Downcomer Boiling Phenomena During the Reflood Phase of a Postulated Large-Break LOCA in the APR1400,” *Nuclear Technology*, **156** (2006).

Zeitoun, O.M., *Subcooled flow boiling and condensation*, Ph. D. Thesis, McMaster University, Canada (1994).